Preliminary Experiments in Visual Servo Control for Autonomous Underwater Vehicle

Chanop Silpa-Anan, Thomas Brinsmead, Samer Abdallah* and **Alexander Zelinsky**
Robotic Systems Laboratory
Department of Systems Engineering
Australian National University, Canberra, ACT 0200, Australia
{chanop|thomas|samer|alex}@syseng.anu.edu.au, http://www.syseng.anu.edu.au/rsl/

Abstract

We are developing a visually-guided autonomous underwater vehicle. We have achieved a position-based visual servo control of fixed and slow moving targets using visual position feedback and sensor-based orientation feedback. The visual position feedback has been implemented on a stereo camera system. We use a compass and an inclinometer for orientation feedback. We have also implemented a computed torque controller using Euler parameters to represent the orientation state, for vehicle motion control. Using Euler parameters eliminates singularities in the model and the controller. Preliminary experimental results of visual servo control are reported.

1 Introduction

At the Robotic Systems Lab, Australian National University, we are developing a visually-guided autonomous underwater vehicle (AUVs) for exploration and inspection tasks[6; 7].

Australia has an extensive coastline and near-shore waters that contain vast biological and mineral resources. These areas are largely unexplored. They must be investigated and understood so that they can be wisely developed and properly protected. In commercial applications, e.g. inspection of underwater cables, pipes, and structures, the cost of operations can be quite high and it might be risky for human in some situations.

Underwater vehicles are becoming more involved in underwater operations. Autonomous underwater vehicles are useful in several kinds of task where some degree of autonomy is desirable. For example, the ability to autonomously maneuver from point to point, the ability to locate and track targets, and the ability to be programmed and to execute such programs in sequence, will enable AUVs to perform many kinds of tasks such as: to search in regular pattern, to follow fixed natural and artificial features, and to swim after dynamic targets. With these capabilities, AUVs could be used in missions such as cataloging reefs, exploring geologic features, studying marine creatures, or inspecting pipes, cables, and underwater structures, as well as assisting human divers.

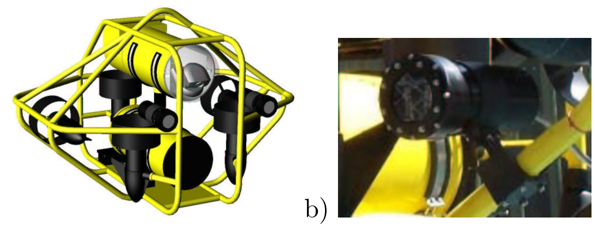

a) b)

Figure 1: a) *Kambara*, the autonomous underwater vehicle at the Robotic Systems Lab, ANU. b) Camera mounted in a water–tight enclosure.

Our vehicle is named *Kambara*[1]. The main research focus for *Kambara* is to use visual information for vehicle navigation. This paper presents preliminary results in visual servo control which is one part of the navigation system. The results show that *Kambara* can visually servo with targets. With a fully functional visual navigation system, we envision that platforms similar to *Kambara*, during operations, will occasionally receive supervisory commands such as "keep station with this reef", "stay here", or "follow the diver".

In this paper, we present the experimental results on visual servo with fixed and moving targets. The vehicle control system and the visual position feedback are described. Implementation and design of *Kambara*'s hardware and software architectures are also presented. Finally, the conclusions and future work are presented.

2 *Kambara* Underwater Vehicle

The design of *Kambara*'s hardware can be classified into two categories: mechanical and electrical.

2.1 Mechanical Structure

Kambara is an open frame AUV (see Figure 1). Its frame supports two main enclosures, five thrusters, and stereo cameras mounted in water-tight enclosures. The vehicle size is 1.2 m × 1.5 m × 0.9 m in length, width, and height. The total mass is approximately 117 kg with all the equipment needed for on–board operations including the battery pack.

*The author is currently at the Faculty of Engineering and Architecture, American University of Beirut.

[1] Australian Aboriginal word for crocodile

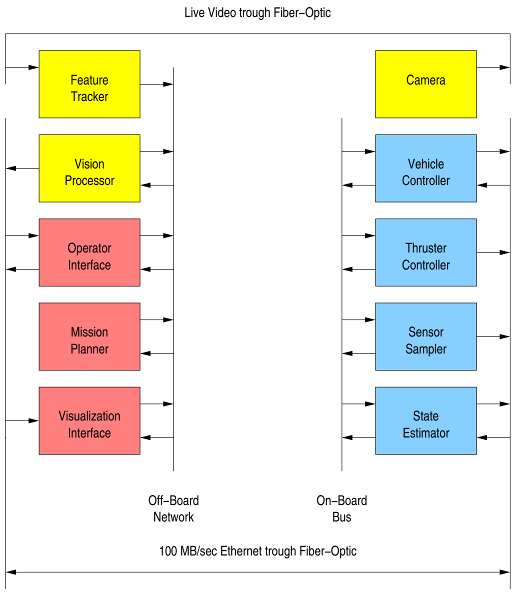

Figure 2: Software architecture of on-board and off-board modules.

Kambara has five thrusters mounted in a configuration that enables five degrees of freedom in motion, namely surge, heave, roll, pitch, and yaw, but not in sway (lateral motion). *Kambara* does not have any thruster that can produce thrust in such a direction. The thrusters are built from commercially available electric trolling motors. The propellers have been cut. Ducts have been added to improve the thrust output. These thrusters are driven by custom-built voltage PWM amplifiers which receive a PWM signal from the *Motorola 68332* CPU.

2.2 Computer and Electronic Devices

The main computing unit is a 233 MHz *PowerPC* processor on a compact PCI board. Accessories include an *Imagenation PXC–200F* video frame grabber, a 100 Mbit/second Ethernet board, and Industry Pack carrier boards holding digital and analog I/O, serial ports, and a *Motorola 68332* CPU. These are mounted in the upper enclosure. Also mounted in the upper enclosure are a *Sony EVI–D30* pan–tilt–zoom camera, a compass, a biaxial inclinometer, a triaxial accelerometer, a rate–gyroscope, a temperature sensor, and a DC-DC power supply. The upper enclosure has a clear front dome for the *Sony* pan–tilt–zoom camera. The lower enclosure houses a 24 V lead–acid battery pack, a depth sensor, and water leakage sensors.

For vision sensing, we have equipped *Kambara* with stereo cameras mounted in water–tight enclosures (see Figure 1.b). These cameras, used for estimating the range of targets, are *Kambara*'s major source of visual feedback. These cameras are small 1/3" CTTV cameras with 2.8 mm lenses. This combination gives a field of view of approximately 86 degrees. When the cameras are submerged underwater, the effective focal length is about 3.9 mm and the field of view is reduced to about 75 degrees. Video signals from these cameras are digitized on–board using an on–board video frame grabber, however, during the development stages, these video signals were processed off–board. There is also a pan–tilt–zoom camera mounted inside the clear dome inside the top enclosure. This is an auxiliary camera for general purpose usage such as the close inspection of an object by zooming.

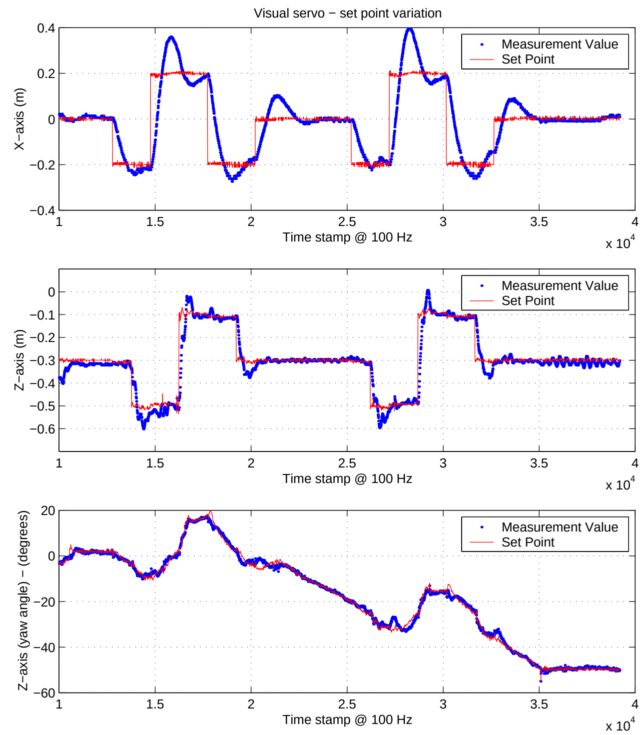

Figure 3: Experimental result in visual servo on a fixed target. This figure shows result of movements in square on **x–z** plane as illustrated in Figure 4.

2.3 Software Architecture

During the development of the visual servo control system, we employed a distributed computing system approach. Figure 2 shows the software architecture used during this development. We have a removable fiber–optic tether, which is attached to the rear of *Kambara*'s top enclosure, and which transmits three video signals from the on–board cameras and also carries a 100 Mbit/second Ethernet link. This fiber–optic link allows us to use a remote machine for vision processing, which is more suitable for developing and monitoring visual feedback than processing the visual information on–board. Using off–board computing for vision pro-

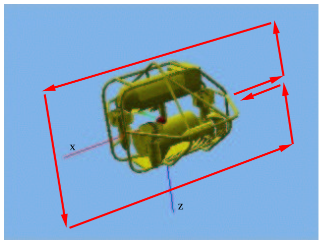

Figure 4: Diagram of the visual servo experiment (Figure 3) in square movements on **x-z** plane.

cessing allows us to use user–friendly real–time GUI tools in developing and debugging the visual feedback algorithm which is not viable with on–board OS, *VxWorks*. Now that visual feedback is working reliably, the vision processing will be moved to the on–board processor, hence, the fiber–optic video link is no longer needed for video signals. When *Kambara* achieves overall reliable autonomous performance, the fiber–optic tether may be removed completely. The high bandwidth Ethernet communication between *Kambara* and the operators will be replaced by a low rate acoustic link.

3 Feedback Signal

There are two main feedback signals for vehicle motion control, a visual position feedback and a sensor-based attitude feedback.

3.1 Visual Position Feedback

We are working with a calibrated stereo camera system on *Kambara*. For *Kambara*, there are some (foreseen) difficulties in calibrating cameras underwater as well as in the vision processing of underwater images. The first difficulty is an image quality problem, since the contrast of an underwater image is fairly low. Image contrast is affected by depth, sediment in the water, and light diffraction. The image quality problem affects both the calibration algorithm and the vision processing.

One other difficulty is an image distortion problem. We use a wide angle lens for the stereo cameras in order to have a large field of view. Image distortion is, however, a common problem for wide angle lenses especially at the corners and around the edges. Due to the image distortion effect, the same object in different images from the stereo cameras can appear quite different.

We have developed and implemented a robust camera calibration algorithm for calibrating underwater stereo cameras based on Tsai's camera calibration algorithm.

The visual position feedback information that is returned in our implementation is the 3D range from *Kambara* to targets. The 3D range is estimated by

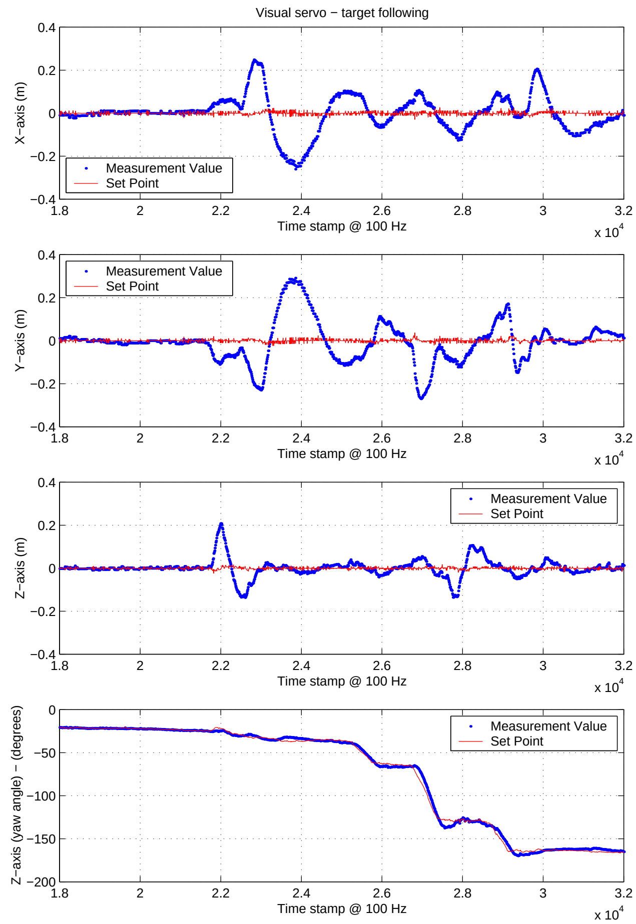

Figure 5: Experimental result in visual servo on a moving target. This figure shows the result of following a target that moves in a circular pool. The diagram of the target movements is illustrated in Figure 6.

a triangulation technique, assuming that the target's location in the stereo images can be found. We have implemented a Normalized Cross Correlation technique for locating targets in stereo images. Normalized Cross Correlation has properties which are matched to the underwater stereo vision problem, e.g. it is robust to differences in illumination and it has bounded output value, -1 to 1. Normalized Cross Correlation performs better when compared to other popular area–based correlation techniques such as sum of absolute difference or sum of square difference. The same target, when viewed from different angles, from different depths, or from different cameras, is likely to have different illumination, therefore, robustness of the algorithm to illumination difference is highly desirable.

Normalized Cross Correlation, however, is quite computationally expensive, but this can be compensated for by optimizing the calculation algorithm or using a faster CPU. The formula for normalized Cross Correlation is given by,

$$\text{NCC} = \frac{\sum (I_1 - \bar{I}_1) \cdot (I_2 - \bar{I}_2)}{\sqrt{\sum (I_1 - \bar{I}_1)^2 \cdot \sum (I_2 - \bar{I}_2)^2}},$$

where NCC is Normalized Cross Correlation value, I_1 is template image, and I_2 is image region of interest. Note that these images are intensity images.

Area–based correlation techniques may suffer from the features of interest changing appearance. This can result from changes in the relative position and orientation between the cameras and the targets. There are several techniques that may be used to address this problem, e.g. using an adaptive template or using multiple templates. This topic is, however, beyond the scope of this paper.

The information about features provides 3D position feedback to the vehicle motion control system. If the target features that are selected are fixed features, this will provide the vehicle with an absolute position and absolute velocity, as well as the relative measures with respect to the features. For a moving target, only relative position and relative velocity between the vehicle and the target can be provided. In the case of following a moving target, knowing only the relative position and relative velocity is quite adequate for tracking purposes. The absolute velocity of either the vehicle or target or both, however, may help in reducing the tracking error due to potential to more accurately model the relative motion dynamics.

The visual feedback scheme presented here has been reported before in visual servo control applications for robot manipulator [1].

3.2 Attitude Feedback

Attitude feedback is implemented by using the compass and biaxial inclinometer sensors. The compass gives a heading reading with respect to the earth's magnetic field. The biaxial inclinometer gives the pitch and roll angles of the vehicle z-axis relative to the earth's gravity vector. These two sensors, when fused together, provide feedback regarding the vehicle orientation relative to the earth-fixed reference frame.

3.3 Fused Sensor Feedback and Vehicle Degree of Freedom

After we fuse the visual position feedback and attitude orientation feedback together, we are able to control the orientation of the vehicle in the earth-fixed reference frame and are able to track the target in the *Kambara* reference frame.

In the case of tracking one target (feature), which is the case for the experimental results presented in this paper, no matter whether it is a fixed or a moving target, the number of degrees of freedom of the target is always three: a relative position between the target and vehicle. *Kambara* has five degrees of freedom in motion and, therefore, two degrees of freedom are redundant in terms of controlling to a relative position between the target and vehicle. We set two more constraints, keeping the pitch and roll angles constant, according to vehicle's natural equilibrium (it is bottom heavy). These redundancies may alternatively be dealt with by adopting trajectory planning techniques

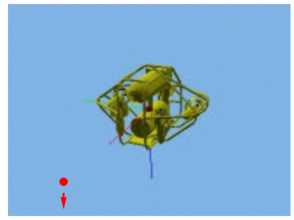

Time stamp $\sim 22 \times 10^3$.

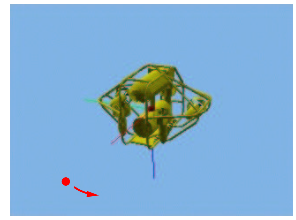

Time stamp $\sim 23 \times 10^3$.

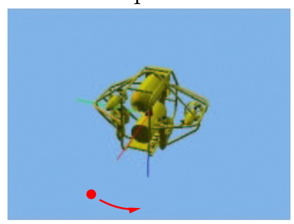

Time stamp $\sim 25 \times 10^3$.

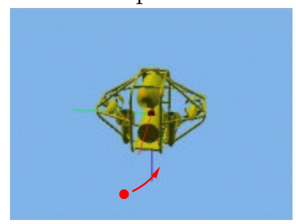

Time stamp $\sim 27 \times 10^3$.

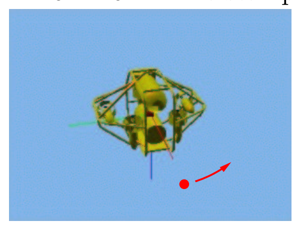

Time stamp $\sim 29 \times 10^3$.

Figure 6: Diagram of target movements in a circular pool for the visual servo experiment (Figure 5) on tracking a moving target.

4 Vehicle Position Control

We have developed a dynamic model for *Kambara* and a computed torque controller for motion control[5]. The vehicle model can be summarized as follows.

$$M\dot{\mathcal{V}} + C(\mathcal{V})\mathcal{V} + D(\mathcal{V})\mathcal{V} + g(\mathbf{q}) = \mathcal{T},$$

where M is a mass and inertia matrix, including hydrodynamic added mass and inertia, $C(\mathcal{V})$ is a Coriolis and centripetal matrix, including hydrodynamic added Coriolis and centripetal mass and inertia, $D(\mathcal{V})$ is a hydrodynamic damping matrix, $g(\mathbf{q})$ is a gravity and buoyancy force and moment vector, $\mathcal{T}$ is a force and torque input vector, $\mathcal{V}$ is a velocity state vector, and $\mathbf{q}$ is an Euler parameter representation of attitude.

We have come up with estimates of *Kambara*'s matrices M and C, and the vector g, both for simulation studies and controller design, by using *Pro Engineer* CAD/CAM software to model the vehicle.

The matrix D is quite troublesome to obtain. One good approximation of D, assuming that *Kambara* operates normally at low speeds, is obtained from a quadratic drag model. We have estimated the matrix D empirically by fitting vehicle motion (velocity and distance) data to time data.

In our implementation of the visual feedback control system, we use attitude feedback from the compass and biaxial inclinometer. Vision is used for position feedback. The implementation of an inertial navigation system is also under development. We have chosen a computed torque controller, specifically a PID plus gravity compensator, to implement the vehicle motion control. Gravity compensation is quite handy for compensating unbalanced forces and moments from the buoyancy and gravity forces. The implemented control law is as follows,

$$\mathcal{T} = \alpha \mathcal{T}' + \beta,$$

where $\alpha = M$, $\beta = g(\mathbf{q})$, and $\mathcal{T}'$ implements the PID tracking control law as,

$$\mathcal{T}' = k_v \dot{\varepsilon} + k_p \varepsilon + k_i \int \varepsilon,$$

where $\dot{\varepsilon} = \mathcal{V}_d - \mathcal{V}$, is the velocity error vector in the *Kambara* reference frame, and $\varepsilon = {}^K\mathcal{P}_d - {}^K\mathcal{P}$, is the position error vector in the *Kambara* reference frame.

Note that the *Kambara* reference frame is the body–fixed reference frame that moves with *Kambara*.

The computed force and torque vector, $\mathcal{T}$, is to be converted into a thrust in thruster space. *Kambara*'s five thrusters produce an input force and torque to drive the system dynamics according to,

$$\mathcal{T} = L\mathcal{U},$$

where $\mathcal{U}$ is a thrust output vector from thrusters, and L is a thrust mapping matrix depending on the geometry of the thruster locations and direction.

The inverse problem of finding the thrust vector, $\mathcal{U}$, from the computed force and moment vector, $\mathcal{T}$, can be approached by using the left pseudo inverse of L as,

$$\mathcal{U} = L^{\dagger}\mathcal{T}, \text{ where } L^{\dagger} = (L^{\top}L)^{-1}L^{\top}.$$

Note that $L \in \mathbb{R}^{6\times5}$, $L^{\dagger} \in \mathbb{R}^{5\times6}$, and if there is any required force in sway direction, it will be neglected since *Kambara*'s thrusters cannot produce thrust in such a direction.

5 Preliminary Experimental Results

We have implemented the system described above on *Kambara* for visual servo control experiments. There are two sets of visual servo control experiment: visual servo on a fixed target and visual servo on a moving target.

5.1 Visual Servo on a Fixed Target

For visual servo on a fixed target, we use a fixed target as a reference point and let *Kambara* move around the reference point. Figure 3 shows the experimental results in moving relative to the fixed target in the **x**–**z** plane. *Kambara* moves in a square of size 40×40 cm as illustrated in Figure 4.

In this experiment, *Kambara* can track the target and move around it according to the pre–defined set points in the **x**–**z** plane using visual position feedback and sensor–based attitude feedback.

Since *Kambara* cannot move directly in the **y**–axis, if there is any error in the **y**–axis, it is compensated by yawing (turning) *Kambara* around the **z**–axis instead. Because of this problem, *Kambara* was drifting slowly to it's right side during the experiment (positive **y**–axis), due to disturbances and some inaccuracies of the system model. Compensation for error in the **y**–axis by turning in the **z**–axis has been made as seen in the graph of yaw angle in Figure 3.

Note that the controller used for this experiment was not optimized, therefore, it shows some characteristics, such as quite large overshoot (∼40%) and slow settling time (∼10 seconds), which could be improved.

5.2 Visual Servo on a Moving Target

For this experiment, we use a moving synthetic fish as a target for tracking. The objective of *Kambara* is to both track the target and to maintain the distance between itself and the target. Figure 5 shows the experimental results in following a target. The set point (relative distance between *Kambara* and the target) is kept constant. The target step movement resembles an impulse input to the system.

The movements of the target in this experiment are described as follows; the target starts moving downward slightly, then slowly to the left of the vehicle; speed increases at time stamp $\sim 25 \times 10^3$, followed by a short pause; there is one big movement to the left followed by a pause and finally, another movement to the left.

In this experiment *Kambara* can visually track and follow the target. The settling time of the system is about the same as the settling time from the visual servo experiment on a fixed target.

Video clips of the experiments can be found at `http://www.syseng.anu.edu.au/rsl/`

5.3 Discussion of Results

Several researchers have been focusing on using vision with AUV. Some of these researches are reported in [2; 4; 3]. Our system can be classified as direct position–based visual servo structure[1] for linear position control. Our results show that reliable visual feedback is achievable and can be used as a major feedback signal for controlling vehicle position. The system can do a station–keeping task as well as target following using the same controller scheme.

The PID plus gravity compensator controller used in this experiments has not yet been optimized for its performance. Therefore the experimental results show a long settling time and quite large overshoot characteristics. This controller could be improved by many means, e.g. an in–depth analysis of the system model or empirical tuning of the controller. A more sophisticated control scheme, such as adaptive control, sliding control, and learning control, however, may be investigated for a better control performance.

In these experiments, only three degrees of freedom have been controlled, surge, heave, and yaw. Rolling and Pitching are kept constant (at zero degrees) according to vehicle's natural equilibrium. The vehicle movement in the **y**-axis is currently compensated by motion in yaw, however, these two motions could be combined with path planning techniques to give the vehicle smooth motion to a target.

6 Conclusion

In this paper, we have shown, in the experimental results, that the *Kambara* AUV can perform visual servo control on fixed and slow moving targets. The visual servo structure implemented uses direct visual feedback for position control. The resulting system has good performance in tracking and following a target.

We have also presented the design of software and hardware architecture for the *Kambara* AUV which is geared towards visual navigation. The concept design, using a distributed computing system for developing the visual servo control has proved to be very useful.

A system model using Euler Parameters to represent attitude has been briefly reported as well as a proposed computed torque controller, specifically a PID plus gravity compensator, for controlling the vehicle in visual servo control. The gravity compensation helps balancing the forces and moments from gravity and buoyancy. This controller has shown a good performance in the experiments, however, it may be improved. Only two feedback signals, visual position feedback and sensor–based attitude feedback, have been implemented for use with the controller.

Visual position feedback has been implemented using Normalized Cross Correlation for locating and tracking the target with the stereo camera system. This well–proven technique has shown a reliable performance in tracking a target underwater.

7 Future Work

Future work for visual servo control for *Kambara* is as follows,

- Extend the visual feedback such that it provides multiple target tracking, orientation feedback, improvement in speed and robustness.
- Improve the speed and robustness of the vehicle controller,
- and Implement the inertial navigation system as a backup system when visual servo is not viable.

8 Acknowledgements

A lot of thanks should go to Dr. David Wettergreen[2] who pioneered this project while he was a research fellow at the robotic systems lab, ANU, and Peter Brown who has devoted a great support to the project.

References

[1] Peter I. Corke, Seth Hutchinson, and Greg D. Harger. A tutorial on visual servo control. *IEEE Transaction on Robotics and Automation*, 12(5):651–670, 1996.

[2] Stephen D. Fleischer and Stephen M. Rock. Experimental validation of a real-time vision sensor and navigation system for intelligent underwater vehicles. In *Proceedings of 1998 IEEE International Conference on Intelligent Vehicles*, October 1998.

[3] Nuno Gracias and José Santos-Victor. Underwater video mosaics as visual navigation maps. *Computer Vision and Image Understanding*, (79):66–91, 2000.

[4] J.F. Lots, D.M. Lane, E. Trucco, and F. Chaumette. A 2-D visual servoing for underwater vehicle station keeping. In *Proceedings of the IEEE International Conference on Robotics and Automation*, pages 2767–2771, Seoul, Korea, May 21-26 2001.

[5] Chanop Silpa-Anan, Samer Abdallah, and David Wettergreen. Development of autonomous underwater vehicle towards visual servo control. In *Proceedings of the Australian Conference on Robotics and Automation*, pages 105–110, Melbourne, Australia, August 2000.

[6] David Wettergreen, Chris Gaskett, and Alex Zelinsky. Development of a visually-guided autonomous underwater vehicle. In *Proceedings of IEEE OCEANS '98 Conference*, Nice, France, September 1998.

[7] David Wettergreen, Chris Gaskett, and Alex Zelinsky. Autonomous guidance and control for an underwater robotic vehicle. In *Proceedings of the International Conference on Field and Service Robotics (FSR'99)*, Pittsburgh, USA, September 1999.

[2] Dr.Wettergreen is currently at the robotics institute, Carnegie Mellon university.